Energy efficient gas phase electrolysis of hydrogen chloride

Simon Bechtel[a], Tanja Vidakovic-Koch[a], Kai Sundmacher[a,b,*]

Hydrogen chloride is a byproduct in important processes like the polyurethane production. The currently most efficient electrochemical process for recycling it to chlorine is based on a liquid phase reactor, utilizing aqueous hydrochloric acid as a feedstock. Recent investigations showed that employing a gas phase reactor and according novel strategies for product purification leads to significant exergetic savings. This article aims to discuss the efficient electrolysis of gaseous HCl on the reactor level but also on the overall process level in comparison to the current state-of-the-art.

Chlorwasserstoff ist ein Nebenprodukt wichtiger industrieller Prozesse wie der Polyurethanproduktion und kann mittels Elektrolyse zu Chlor recycelt werden. Der zurzeit effizienteste industriell genutzte Prozess verwendet Salzsäure als Edukt und basiert auf einem Flüssigphasenreaktor. Jüngste Untersuchungen haben gezeigt, dass die Verwendung eines Gasphasenreaktors und neuartiger Separationsstrategien zur Produktaufreinigung zu signifikanten Exergieeinsparungen im Vergleich zu dem State of the Art Prozess basierend auf dem Flüssigphasenreaktor führen. In diesem Beitrag wird die energieeffiziente Elektrolyse von gasförmigem HCl auf Reaktor- und Prozessebene diskutiert und mit dem State of the Art Prozess verglichen.

Keywords

Energy-Efficient HCl Oxidation, Gas Phase Electrolysis**,** Chlorine Recycling, Process Evaluation

Author Affiliation

[a] Max Planck Institute for Dynamics of Complex Technical Systems, Department Process Systems Engineering, Sandtorstr.1, D-39106 Magdeburg, Germany

[b] Otto-von-Guericke- University Magdeburg, Department Process Systems Engineering, Universitätsplatz 2, D-39106 Magdeburg, Germany

* Corresponding author: sundmacher@mpi-magdeburg.mpg.de

Introduction

Chlorine is a base chemical used in the production of various substances including polymers, solvents, disinfectants and many more [1,2]. Its production capacity was at 66 million metric tons per year in 2014 and from there is expected to increase by 10 million tons until 2019 [3]. It is noteworthy that 50 % of the chlorine used for the production of chemicals is being discharged in the form of side products like hydrogen chloride or chloride salts and one third of the final products do not contain Cl_2 themselves [4]. Amongst those are isocyanates and polycarbonates whose production is of high industrial significance [4]. In 2013, the worldwide capacity of polycarbonates was at 3.7 million tons and is predicted to increase by 5% until 2018 [4]. The most important isocyanate is methylen diphenyl diisocyanate (MDI) with a production capacity of 4.6 million tons in 2011 and a growth rate of 5%, followed by toluene diisocyanate (TDI) with a production volume of 3 million tons in 2013 [1,5,6,7]. Both, the isocyanate and polycarbonate production utilize phosgene as a reactant, which itself is obtained from the reaction of chlorine and carbon monoxide. Hence, for each produced mole of TDI and MDI, two moles of chlorine are consumed and four moles of hydrogen chloride accrue as a byproduct. On the other hand, hydrogen chloride consuming processes, like the production of PVC, are growing at a much slower rate, leading to an over-saturation of the hydrogen chloride or hydrochloric acid market [2,4]. The electrochemical recycling of chlorine by electrolysis of hydrogen chloride as depicted in (Fig. 1), offers a sustainable solution to this problem.

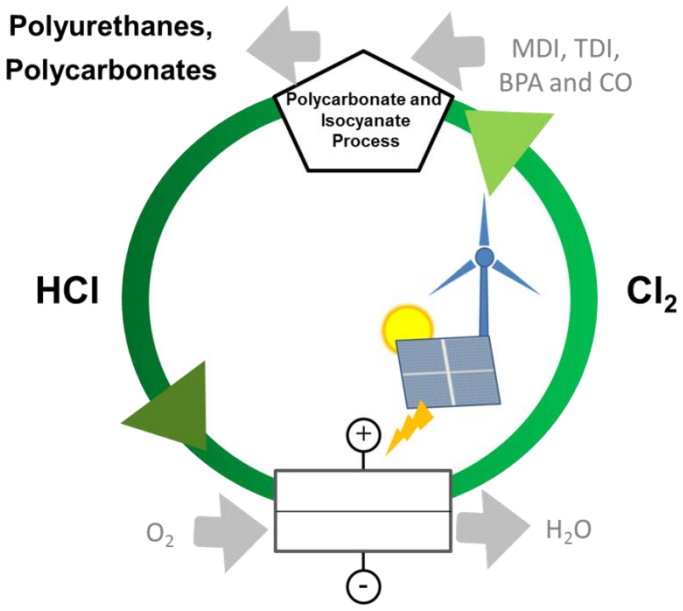

Figure 1. Utilization of electrical energy, for example from renewable sources, for the electrolysis of gaseous HCl emerging from processes like the isocyanate and, for certain process variants, the polycarbonate production. The obtained chlorine can then be refed into these production processes. Reprinted from [7] with permission from Elsevier B.V.

The electrochemical recycling of chlorine from HCl was already developed in 1948 and industrially employed from the 1960s on in the form of the Bayer-Uhde-Höchst process based on the diaphragm electrolyzer technology [8]. It utilizes aqueous hydrochloric acid as a reactor feed. In the cathode chamber, hydrogen is produced, following the overall stoichiometry depicted in (Eq. 1):

$$\boldsymbol{Overall}: \quad \mathbf{2HCl_{(aq)} \rightarrow Cl_{2(g)} + H_{2\,(g)}} \tag{1}$$

$$Cathode: \quad 2H^+_{(aq)} + 2e^- \rightarrow H_{2\,(g)}$$

$$Anode: \quad 2HCl_{(aq)} \rightarrow Cl_{2\,(g)} + 2H^+_{(aq)} + 2e^-$$

A more recent process variant was proposed by Bayer, from which Covestro emerged in 2015, Thyssenkrupp Uhde Chlorine Engineers as well as Industrie De Nora, from now referred to as the Bayer UHDENORA process [10]. It is based on the membrane electrolyzer technology employing an oxygen depolarized cathode (ODC), which reduced the energy consumption of the electrochemical reactor by 30 % [2,4,5]. Hence the overall stoichiometry reads as follows:

$$\textbf{\textit{Overall}}: \quad \mathbf{4HCl_{(aq)} + O_{2\,(g)} \rightarrow 2Cl_{2(g)} + 2H_2O_{(l)}} \tag{2}$$

$$\textit{Cathode}: \quad O_{2(g)} + 4H^+{}_{(aq)} + 4e^- \rightarrow 2H_2O_{(l)}$$

$$\textit{Anode}: \quad 4HCl_{(aq)} \rightarrow 2Cl_{2(g)} + 4H^+{}_{(aq)} + 4e^-$$

The Bayer UHDENORA process is also based on a liquid phase reactor utilizing hydrochloric acid as a feed and is the up to now most efficient industrially employed electrochemical process variant. In order to highlight the conceptual differences between this state-of the-art process and the in (Sect. 2) introduced novel process based on a gas phase reactor and according separation strategies, a flowsheet of the Bayer UHDENORA process is depicted in (Fig. 2) [7].

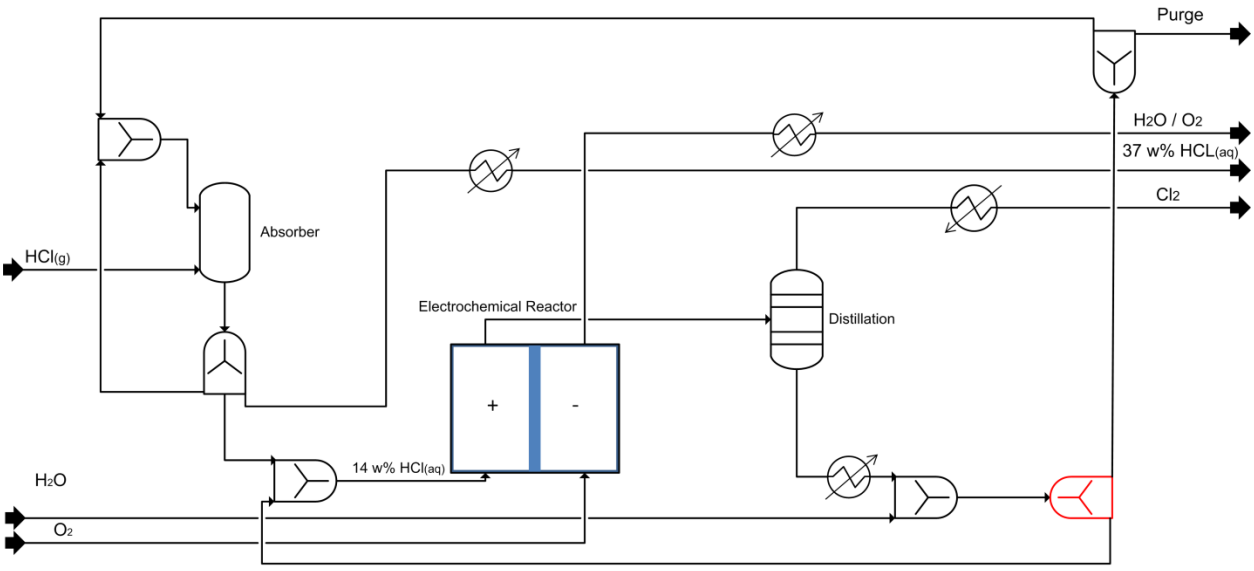

Figure 2. Process flowsheet of the Bayer UHDENORA process. Reprinted from [7] with permission from Elsevier B.V.

The incoming gaseous hydrogen chloride is absorbed in diluted hydrochloric acid forming concentrated hydrochloric acid. Part of this stream can be discharged from the process as a desired side product. The remaining part is diluted to a concentration of ca. 14 w% and fed into the electrochemical reactor, where chlorine is emerging as a product, leaving the anode chamber of the reactor together with the unreacted hydrochloric acid whose concentration is now at ca. 11 w% [10]. Subsequently, the chlorine is separated in a distillation column and the remaining

diluted acid is fed into the absorber to absorb newly incoming hydrogen chloride. Bechtel *et al.* [7] have shown that one of the major problems of this process is the low possible single pass conversion of only 23 %, which is limited by a decrease in the electric conductivity of the solution and the ionomer at higher hydrochloric acid concentrations in the feed and the oxygen evolution reaction taking place if the hydrochloric acid concentration is too low [11]. As a consequence, the recycle streams in the process are of enormous size, especially when a high overall conversion rate is desired. This does not only lead to the necessity of larger devices and therefore higher material costs but also a high energy demand in the distillation column due to the great amount of diluted acid that has to be boiled. The latter problem is even amplified owing to the high heat capacity of the acid solution which makes the separation step very energy inefficient. For a detailed exergy analysis and a more exhaustive description of the Bayer UHDENORA process, the reader may refer to [7]. Owing to these inefficiencies of the current state-of-the-art, there have been efforts in recent years to develop a novel and more energy efficient reactor and overall process for the industrially highly relevant electrolysis of hydrogen chloride. In this novel reactor, HCl is employed as a gaseous reactant, leading to markedly lower cell potentials and allowing for a more energy efficient separation strategy.

1. Direct electrolysis of gaseous HCl

1.1 Different concepts for gas phase reactors in the scientific literature

The first gas phase reactor that was attempted to be industrially applied was proposed in the US patent 5411641 A from Dupont in 1995 [12]. While gaseous hydrogen chloride is converted to chlorine in the anode compartment of the cell, the protons diffusing though the proton exchange membrane are reduced to form hydrogen at the cathode. Even though investigated on a pilot scale, this process was never industrially commercialized. Recently, Kuwertz *et al.* [13] and Martinez *et al.* [19] developed a gas phase reactor in which the anode reaction is equivalent to the one proposed by Dupont, for the cathode reaction however, an ODC is employed. Hence, oxygen and the protons permeating through the membrane are forming water at the cathode catalyst. The use of an ODC greatly reduces the cell potential [13]. A disadvantage however, consists in the more sluggish oxygen reduction and more difficult water management in comparison to the hydrogen evolution reaction, which restricts the practical operation to lower, but still technically feasible current densities. The cell voltage of the reactor proposed by

Kuwertz *et al*. [13] is -0.97 V at a current density of 4 kA m^{-2} and a temperature of 40 °C compared to cell voltage values ranging from -1.4 to -1.7 V for the Dupont reactor at the same current density depending on the temperature, catalyst material and mode of operation as can be extracted in detail from [12]. Recently, Zhao *et al*. [14,15] proposed two alternative cathode reactions employing a Fe^{2+}/Fe^{3+} and I_3^-/I^- redox mediation [14,15]. A similar approach, however for the electrochemical treatment of organic waste is described by Tatapudi *et al.* [16]. The respective ion being reduced through the electrochemical reaction is oxidized by feeding gaseous oxygen into the catholyte tank and thereby regenerated to again take part in the electrochemical reaction. The advantage of this mediation system is a low cell voltage of 0.64 V for the Fe^{2+}/Fe^{3+} pair and 0.94 V for the I_3^-/I^- pair at 4 kA m^{-2}. Additionally, no expensive catalyst is needed. However, a major disadvantage turned out to be the significant performance decay rate. After an operation time of 80 h in the Fe^{2+}/Fe^{3+} case and only 17 h in the I_3^-/I^- case, the cell voltage rose to almost 1.2 V [14,15]. The prominent decay is most likely due to the presence of cations which strongly reduce the proton conductivity of the membrane. Even in the I_3^-/I^- system, it can be assumed that the decay is a consequence of the counter ion K^+, as Hongsirikarn *et al.* [17] have shown that not only iron cations but also Na^+ significantly reduces the membrane conductivity. The observed increase in the cell potential to 1.2 V at 4 kA m^{-2} in the experiments of Zhao *et al.* is in good agreement with the expected membrane overpotential due to the presence of cations based on the work of Hongsirikarn *et al.* This substantial decay rate makes both reactor variants proposed by Zhao *et al.* [14,15] inapplicable in an industrial process in their current state. For this reason, the present contribution mainly focuses on the gas phase reactor employing an ODC. All three discussed variants of the gas phase reactor are visualized in (Fig. 3).

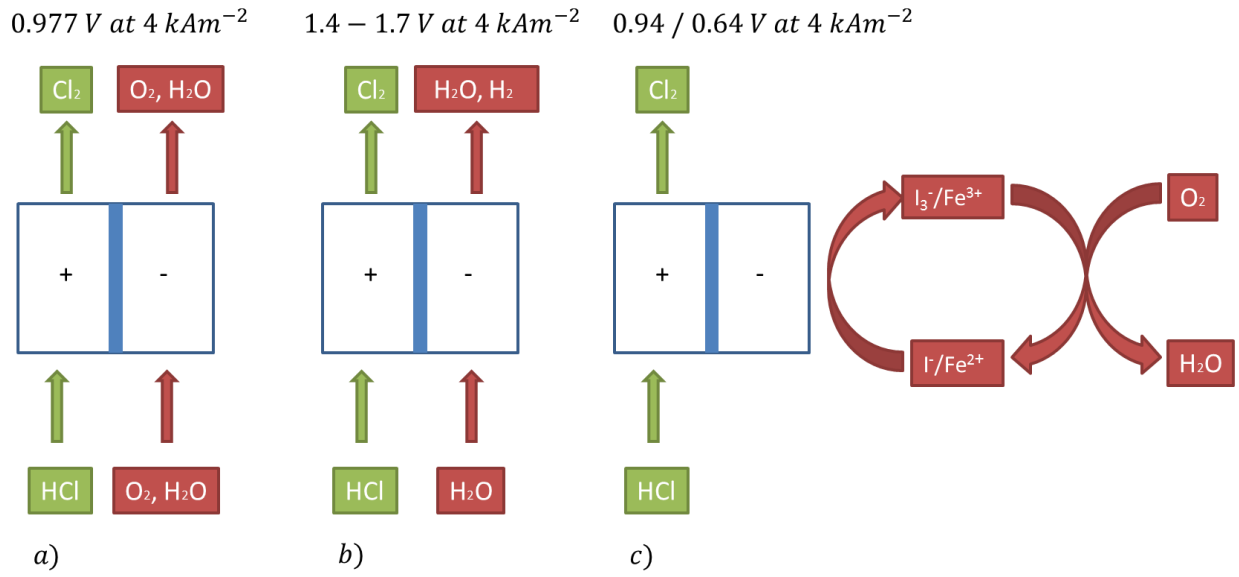

Figure 3. Scheme of the gas phase reactors as proposed by Kuwertz *et al.* [13] (a), Dupont [12] (b) and Zhao *et al.* [14,15,16] (c).

1.2 Thermodynamics of the gas phase reactor

Before going into more detail about the gas phase reactor proposed by Kuwertz *et al.* [13,19] and Martinez *et al.* [22], its thermodynamic characteristics will be briefly introduced and compared to the Bayer-Uhde-Höchst, the Bayer UHDENORA and the Dupont process.

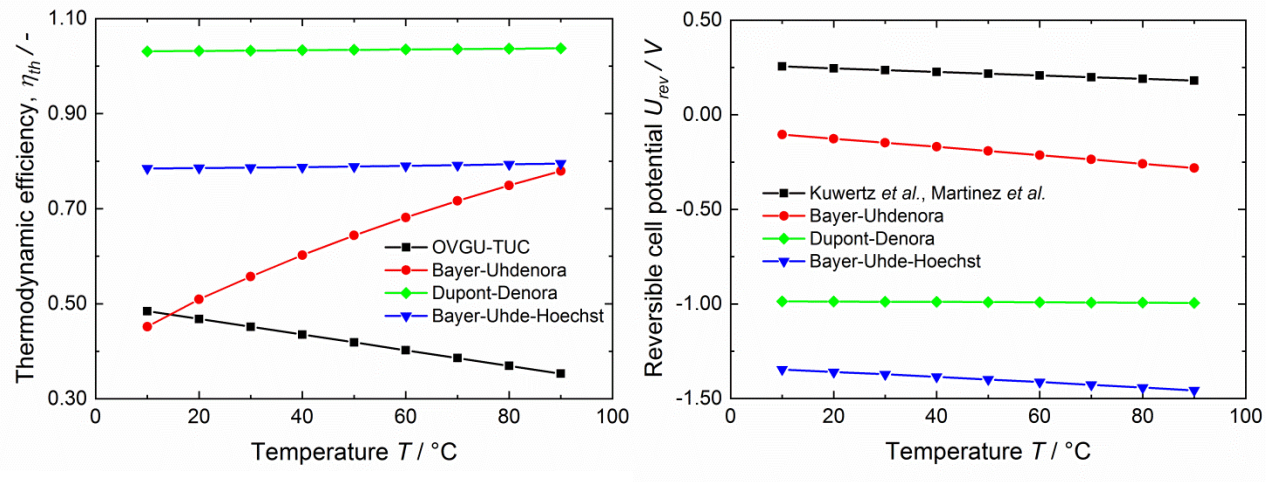

Figure 4. Thermodynamic efficiency (a) and reversible equilibrium cell potentials (b) for the four different discussed HCl electrolysis processes. Adopted from [18] with permission from author.

As can be extracted from (Fig. 4a), the Dupont process has the highest thermodynamic efficiency reaching values of more than one due to the endothermic reaction and the negative reaction entropy. The efficiency is hereby defined as the ratio of the Gibbs free energy of the reaction and the reaction enthalpy. In a realistic temperature interval of 40 to 80°C, the gas phase process employing an ODC shows a thermodynamic efficiency of approximately 45 to 38% respectively. The reversible cell potentials depicted in (Fig. 4b) shows that the process based on a gas phase reactor and an ODC is the only spontaneous one and illustrates the significant energetic advantage of this reactor concept. Its decrease with rising temperature in the case of the reactor type proposed by Kuwertz *et al.* [13,19] and Martinez *et al.* [18,21] is due to the negative reaction entropy of both the anode and the cathode reaction. As Martinez [18] has shown, the temperature dependence of the ORR is hereby more strongly pronounced compared to the HCl oxidation reaction, due to the higher values of the reaction entropies. From a thermodynamic point of view, low temperatures and high reactant concentrations, implying no humidification of the cathode feed, are therefore most beneficial. However, the effect of the temperature on the reaction kinetics and also the water management in the cell has to be taken into account. Furthermore, Bechtel *et al.* [7] have shown that operating the reactor at 80° instead of 40° while assuming a comparable performance would decrease its exergy demand by 18 % due to the higher temperature level of the discharged heat. In addition to the temperature, also the humidification of the cathode stream proofed to be critical for the water management of the cell, leading to overall optimal process conditions that clearly differ from the optimal settings from a purely thermodynamic point of view, as will be further discussed in (Sect. 1.5).

1.3 Design of the electrochemical gas phase reactor employing an ODC

The working principle of the gas phase reactor is visualized in (Fig. 5a) [19]. The HCl entering the anode compartment of the cell diffuses from the serpentine shaped flow field through the gas diffusion layer (GDL) towards the anode catalyst layer (ACL) where it is converted to chlorine. The product chlorine itself diffuses through the GDL towards the flow field and is leaving the reactor together with not converted hydrogen chloride. In a similar manner, the oxygen entering the cathode compartment of the cell is diffusing towards the cathode catalyst layer (CCL) where it is being reduced and is forming water with the protons, which are emerging from the hydrogen

chloride oxidation reaction on the anode side and diffusing through the ionomer membrane in-between the two catalyst layers. Ideally, the membrane is only permeable for protons and water. The latter one being transported form the cathode to the anode through a diffusion mechanism following a concentration gradient and from the anode to the cathode due to the electroosmotic drag caused by the migration of protons through the membrane. The concentration gradient of water is caused by the humidification of the oxygen stream entering the cathode compartment as well as the oxygen reduction reaction in which water is formed. The first reactor based on the above mentioned principles was constructed and operated by Kuwertz *et al.* [19] and their setup is shortly introduced in the following.

As (Fig. 5b) shows, the reactor consists of two end plates made of titanium followed by fluoropolymer gaskets and the bipolar plates with integrated flow fields made out of a graphite-polymer compound. Furthermore, copper current collectors were used (not shown in Fig.5b). The components subsequent to the bipolar plates are the GDLs, which are responsible for the distribution of the reactants and for the removal of the reaction products. The GDLs were made out of carbon cloth coated with polytetrafluoroethylene (PTFE) in a first step and with a mixture of Ketjenblack and PTFE in a second step leading to a three dimensional network consisting of hydrophilic and hydrophobic parts with a microporous structure. The overall PTFE content in the GDL was 20 wt%. In-between the two GDLs of the anode and cathode compartment is the membrane electrode assembly (MEA), which consists of a Nafion® 117 membrane in between the CCL and ACL [13,19]. The catalyst layer consisted of a commercial catalyst from BASF with 60 wt% Pt/C and Nafion [19]. The measurements were performed at two different catalyst loadings: In the first case, 1 mg cm^{-2} Pt and 1 mg cm^{-2} Nafion were chosen on both the anode as well as the cathode side (referred to as standard loading) and secondly, 0.5 mg cm^{-2} Pt with 1 mg cm^{-2} Nafion was chosen for the anode and 0.5 mg cm^{-2} Pt with 0.5 mg cm^{-2} Nafion for the cathode, denoted as optimized loading as explained in (Sect. 1.4) [19,20]. The employed membrane consisted of Nafion 117® and was pretreated with deionized water, hydrogen peroxide and 1 M H_2SO_4 at elevated temperatures [13,19]. The active area of each electrode was 30 cm^2 [13]. For details on the influence of the composition of the GDL and the MEA on the cell performance, please refer to (Sect. 1.5) of this work and to [19].

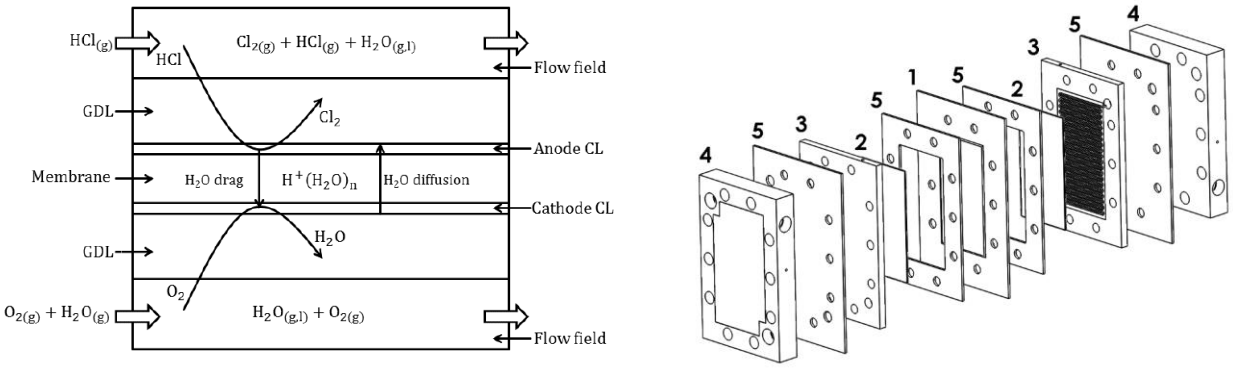

Figure 5. (a) Working principle of the gas phase reactor. Reprinted from [30] with permission from the Electrochemical Society. (b) Explosion view of a gas phase reactor for the hydrogen chloride electrolysis consisting of: One MEA (1), two GDLs (2), two bipolar plates (3), two end plate (4) and the gaskets (5). Reprinted from [19] with permission from Springer Nature.

1.4 HCl oxidation reaction and mechanism in a half cell

The oxidation of hydrogen chloride to chlorine follows the stoichiometry depicted in (Eq. 3) [21]:

$$2HCl_{(g)} \rightarrow Cl_{2(g)} + 2H^{+}_{(aq)} + 2e^{-} \quad (3)$$

If the hydrogen chloride dissolves in the water present in the ACL instead of reacting in its molecular form, the according reaction equation reads as follows [21]:

$$2Cl^{-}_{(aq)} \rightarrow Cl_{2(g)} + 2e^{-} \quad (4)$$

The equilibrium potentials at standard conditions are 0.99 V if HCl reacts in its gaseous state and 1.36 V in case of a prior dissociation according to (Eq. 4) [21]. Martinez *et al.* [21] experimentally determined an open circuit potential (OCP) of 1.03 V, while Eames *et al.* [22], who investigated a similar gas phase reactor for the HCl electrolysis but with hydrogen evolution as the cathode reaction, have identified a value of 0.99, which is closer to standard potential of the gas phase reaction (Eq. 3) [21]. However, low Cl_2 concentrations as well as the high solubility of hydrogen chloride, and the subsequently high concentration of chloride anions in the ACL, can significantly reduce the equilibrium potential of (Eq. 4) and hence, possibly explain the experimentally observed OCP. As will be shown in the course of this section, there are further arguments for the prior dissociation of HCl to chloride anions and protons in the ACL

according to (Eq. 4). Hence, so far it is not possible to determine with certainty, whether the hydrogen chloride dissociates in the water contained in the Nafion of the ACL prior to its conversion to chlorine or not.

In the following, the effect of temperature, the hydrogen chloride concentration and the Nafion as well as the platinum loading in the ACL on the HCl oxidation reaction are briefly discussed. The experimental investigations of Martinez *et al*. [21] showed only a slight temperature dependence of the current-voltage relation, as depicted in (Fig. 6). The difference between the lowest and highest temperature at a technical current density of 400 mA cm^{-2} is ca. 15 mV. The change in the OCV is only 3 mV at the four different temperatures [21]. Due to the higher entropy change in the liquid phase reaction of chloride anions compared to the reaction of gaseous HCl, this weak temperature dependence would be a further indication for the direct oxidation of molecular HCl [21]. However, one has to consider that the activity of chloride anions in Nafion in equilibrium with the hydrogen chloride gas phase at 60° is significantly lower than at room temperature due to the smaller amount of absorbed hydrogen chloride and the temperature dependence of the activity coefficient of $HCl_{(aq)}$ [21]. Hence, Martinez *et al.* [21] concluded that also the temperature dependence of the OCV does not allow for a certain discrimination of either the direct oxidation of molecular HCl or the oxidation of dissolved chloride anions. The same holds for the experimentally determined influence of different HCl gas phase concentrations on the OCV, which differed from the theoretically expectable values for both, the HCl and the Cl^- oxidation. Martinez *et al.* [21] showed that the reaction order is approximately 1 regarding the gas phase concentration of HCl and between 1.37 at low potentials and 1 at higher potentials regarding the activity of chloride anions in the CCL, which will be relevant for the discussion of the reaction mechanism in the course of this section. Please note that in (Fig. 6) the kinetic current density is plotted. If the actual current density is plotted, the Tafel-slope increases further at current densities of ca. 300 mA cm^{-2} and approaches infinitely high values at current densities of 500-1000 mA cm^{-2}, depending on the temperature. Martinez *et al*. have assumed that this limiting current density is due to mass transfer limitations and therefore only plotted the kinetic contribution in their work by correcting for the supposedly mass transfer induced part. However, in the course of this section, indications for the limiting current being an intrinsic consequence of the reaction mechanism and not the mass transport, as

assumed by Martinez *et al.*, will be given. This should be carefully considered when discussing the reaction order and Tafel-slopes determined by Martinez *et al.*

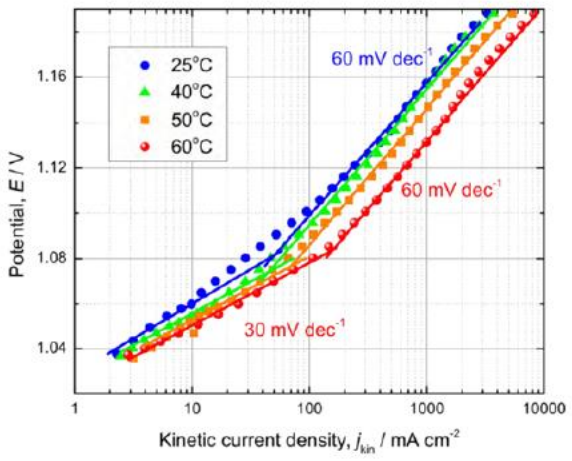

Figure 6. Influence of temperature on the HCl oxidation presented as Tafel plot. For all temperatures, even though less clear at a temperature of 25°C, two different Tafel-slopes of *ca.* 30 mV dec^{-1} at more negative potentials and *ca.* 60 mV dec^{-1} at more positive potentials can be observed [18]. Reprinted from [18] with permission from the author.

For determining the influence of the Nafion loading in the ACL on the cell performance, Martinez *et al.* [18] have investigated three different Nafion contents of 71 wt%, 55 wt% and 38 wt% at a constant platinum loading. Interestingly, the lowest potentials at current densities of up to 500 mA m^{-2} can be achieved with the highest Nafion loading. For the oxygen reduction reaction (ORR), optimal Nafion contents of 30-36 wt% can be found in the literature, which is significantly lower than the optimal values for the HCl oxidation determined by Martinez *et al.* [23,24]. There are various possible explanations for this surprisingly high optimal Nafion loading, one being that if the HCl is absorbed in the water containing Nafion of the ACL, the highly exothermal dissociation reaction leads to an evaporation of water. A higher Nafion content might help in retaining the water in the ACL and subsequent membrane layer which in return would have a positive impact on the proton conductivity and hence the cell performance according to Martinez *et al*. [20]. Furthermore, Martinez *et al.* [20] stated that the mass transfer of HCl through the Nafion in the ACL is significantly faster than the one of oxygen in the CCL due to the better solubility of HCl. While an increase in the Nafion content leads to a higher mass transfer resistance, up to a certain level it also increases the number of active sites, since platinum particles that are not in contact with Nafion, as a consequence of a low Nafion content,

cannot contribute to the reaction. These two effects lead to an optimal value of the Nafion loading. A second possible explanation for this optimal value being higher in the ACL in comparison to the CCL, is therefore the markedly higher solubility and accordingly faster mass transfer of HCl in the ACL.

In addition to varying the Nafion content, the authors showed that reducing the platinum loading from 1 mg cm^{-2} to 0.5 mg cm^{-2} leaving the Nafion loading constant at 0.5 mg cm^{-2} only markedly reduced the performance of the cell at current densities greater than 500 mA cm^{-2}. Hence at technical current densities of ca 400 mA cm^{-2} the platinum loading can be reduced by 50 % compared to the *standard loading* defined in the (Sect. 1.3) of this article without significant losses in the cell performance [20]. This investigation was the basis for the *optimal loading* introduced in (Sect. 1.3).

Martinez *et al.* [21] investigated two possible reaction mechanisms, which are introduced briefly in the following. In the first variant A, two HCl molecules adsorb on the catalyst surface and dissociate leaving two chloride anions adsorbed on the catalyst and two protons emerging. The two adsorbed chloride anions then react to chlorine. In the second mechanism B, the adsorbed chloride ion is reacting with molecular, non-adsorbed HCl to chlorine [21].

$$HCl_{(g)} + Pt \rightarrow PtCl + H^+ + e^- \quad (5)$$

$$2PtCl \rightarrow 2Pt + Cl_{2\,(g)} \quad (A) \quad (6)$$

$$HCl_{(g)} + PtCl \rightarrow Pt + Cl_{2\,(g)} + H^+ + e^- \quad (B) \quad (7)$$

If the HCl dissociates before the electrochemical reaction, the HCl in (Eq. 5) and (Eq. 7) can be simply substituted by Cl^- and the protons on the right side of the equation are taken out of the stoichiometric equation.

Considering the Tafel-slopes depicted in (Fig. 6), mechanism A seems more likely, since it predicts values of ca. 30 mV at low coverages and 60 mV at intermediate coverages. In the case of the surface coverage approaching a value of one, an infinite Tafel-slope in the case of mechanism A and a Tafel-slope of 116-132 mV for mechanism B for temperatures of 20 and 60°C are to be expected [18]. In (Fig. 6), the Tafel-slopes never exceed values of 60 mV. There

are two possible explanations for this. Firstly, it is thinkable that the surface coverage does not reach values close to one in the experiments of Martinez *et al.* There is indeed scientific literature investigating the adsorption of chloride anions on platinum, showing a low to intermediate surface coverage [25, 26]. However it has to be critically considered that their conditions regarding HCl concentration, platinum surface and cell potential amongst others differ clearly from the ones in the experiments of Martinez *et al.* Hence, further research is necessary to precisely evaluate the adsorption behavior under conditions relevant for the gas phase electrolysis process.

Earlier in this section, it was discussed that Martinez *et al.* [18] only considered what they believed to be the kinetic current density in their Tafel plots (please see Fig. 6). However, if mechanism *A* is valid and (Eq. 6) is the rate determining step, the overall reaction rate is limited by the formation and desorption of chlorine, which is a purely chemical reaction step. At the maximum surface coverage, a further increase in the cell potential would therefore not lead to an increase in the reaction rate and accordingly the current density. This is the reason for an expected infinite Tafel-slope in the case of mechanism *A* being valid, which was also observed experimentally by Martinez *et al.* [18]. However, they possibly falsely assumed this infinite Tafel-slope to be due to mass transfer limitations and therefore also possibly falsely disregarded this limiting behavior in their Tafel plots. This is the second potential explanation for why (Fig. 6) only shows Tafel-slopes of up to 60 mV. Only when plotting the measured current density instead of the kinetic one, infinite Tafel-slopes are observed, supporting the reaction mechanism *A*.

The experimentally observed reaction order regarding $HCl_{(g)}$ does not fit any of the two mechanisms. The observed reaction order regarding Cl^- anions however, is comparable to the prediction of mechanism *A*, according to which the reaction order is 2 at low surface coverages and 1 at intermediate coverages. With rising potentials, the experimentally determined reaction order regarding chloride anions decreased from 1.35 to 1. Again, it has to be considered that if the limiting current is not due to mass transport limitations but an intrinsic consequence of the mechanism *A*, the reaction order has to be recalculated using the raw experimental data and not the kinetic current density as done by Martinez *et al.* [21].

Taking the discussed reaction orders and the Tafel-slopes into consideration, it can be summarized that the present available data points towards the mechanism *A* [21]. However, further research is necessary to determine whether the limiting behavior is indeed due to mass transfer limitations or, as discussed above, due to the rate determining second reaction step of mechanism *A*.

Finally, Martinez *et al.* [21] have estimated the contribution of the mass transfer and reaction resistance to the limiting behavior that becomes obvious in their half-cell measurements at current densities of 500-700 mA cm^{-2}, depending on the structure and composition of the ACL. By determining a value for the second Damköhler number of 0.0093 at a current density of 700 mA cm^{-2}, they conclude that the resistance of the electrochemical reaction is markedly higher than the mass transfer resistance in the ACL [21]. However, it should be considered that the ACL consists of agglomerates that contain the active platinum side surrounded by Nafion. The size of these agglomerates is not exactly known but usually is considered to be in the range of a few hundred nanometers [27,28]. Recalculating the second Damköhler number assuming that the reaction is taking place in these agglomerates with an exemplary size of 1 µm and with HCl being dissolved, and therefore employing its liquid phase diffusion coefficient in Nafion of $1.2*10^{-11}$ m^2 s^{-1} [11], leads to values that are approximately 25 times higher. While the resistance of the electrochemical reaction is still dominant in that case, the mass transfer in the agglomerates of the catalyst layer plays a more significant role than assumed before. Literature studies on the ORR have shown that changing the Nafion and platinum loadings in the CCL while keeping their ratio constant did not change the specific current density per catalyst mass [29]. This indicates that the mass transfer resistance mainly comes from within the agglomerate and not the gaseous transport of the reactants in the CL, since the changing catalyst thickness did not influence the performance. This supports the above described finding of a higher resistance of the reactant diffusion within the agglomerate than within the pores of the CL.

Martinez *et al.* [21] furthermore determined the Biot number for relating the mass transfer resistances in the separate layers. When comparing the overall mass transfer resistance in all layers combined to the resistance of the electrochemical reaction, they came to the conclusion that both contributions are comparable [21]. Hence, in any attempt to model the gaseous electrolysis of HCl, careful attention should be paid the mass transport of the reactants in the gas

phase and also the agglomerates, especially in the light of the above discussed higher value for the second Damköhler number within the agglomerates compared to the one for the CL.

To put the relevance of the performance of the HCl oxidation reaction for the overall electrolyzer performance into context, the anode overpotential was 90 mV at a current density of 400 mA cm^{-2} for the best MEA investigated by Martinez *et al*. [20]. While it is important to understand the underlying principles of the HCl oxidation in the ACL, the following section will show that the contribution of the cathode overpotential clearly surpasses the one of the anode, and that effects which concern both the HCl oxidation and ORR simultaneously, like the water management, become decisive for the performance of the reactor at technical current densities. Hence, in the following, the performance of the overall cell in dependence on different parameters and possible explanations for the experimentally observed limiting behaviors will be discussed.

1.5 Role of the ORR and physical effects determining the overall reactor performance

The performance of the overall gas phase reactor combining the HCl oxidation with the ORR seems to be mainly influenced by two effects. The first one being the water management at higher current densities and the second one being the reduced open circuit potential and the activation overpotential of the cathode.

In the experiments of Kuwertz *et al.* [30], the cathode performs significantly worse than in classical hydrogen PEM fuel cells. The measured OCV of the cathode was between 680 and 770 mV and the potential decreased to ca. 130 mV at a low to moderate current density of 3 kA m^{-2} [30]. It is very likely that this reduction in the performance is due to the presence of chloride anions in the CCL caused by crossover from the anode compartment of the cell.

Schmidt *et al.* [31] have shown that a chloride ion contamination of only 4 ppm on the cathode side leads to a voltage loss of 50 mV. They state that increasing the chloride ion concentration by one order of magnitude reduces the catalytic activity of the platinum catalyst by one order of magnitude as well. For this reason, Schmidt *et al.* [31] recommend to not pretreat the Nafion membrane with hydrochloric acid. Investigations from Kuwertz *et al.* [32] on the effect of different acids for the membrane pretreatment, showing that employing hydrochloric acid instead of sulfuric acid lead to a significant increase in the cell potential, support these findings (please see Fig. 7). Furthermore, the chloride ions adsorbed on the platinum surface lead to a strong increase in the H_2O_2 production, since they reduce the number of pairs of Pt-sides that are necessary for the dissociation of the O-O bond and thereby inhibit the complete four electron reduction of oxygen [31]. Katsounaros *et al.* [33] further explain these findings by stating that the presence of certain anions, like Cl^-, can change the ratio between the rate of the H_2O_2 dissociation step and its desorption from the catalyst surface and therefore increase the production of H_2O_2. This does not only have a negative impact on the cell voltage but also leads to a degradation of the Nafion membrane. Moreover, the experimentally observed decrease in the open circuit potential in the experiments of Kuwertz *et al.* [30] is likely to be attributed to the presence of chloride anions on the catalyst surface as well, since Wang *et al.* [34] showed that adsorbed anions can lead to a potential shift for the ORR. Hence, further research in this field should take different catalyst materials like RhS, which is not sensitive to the presence of chloride anions [35], into account and aim at understanding and minimizing the crossover of HCl/Cl_2. The current-cell potential curve for the gas phase electrolysis of HCl extracted from the work of Kuwertz *et al.* [19] is depicted in (Fig. 7).

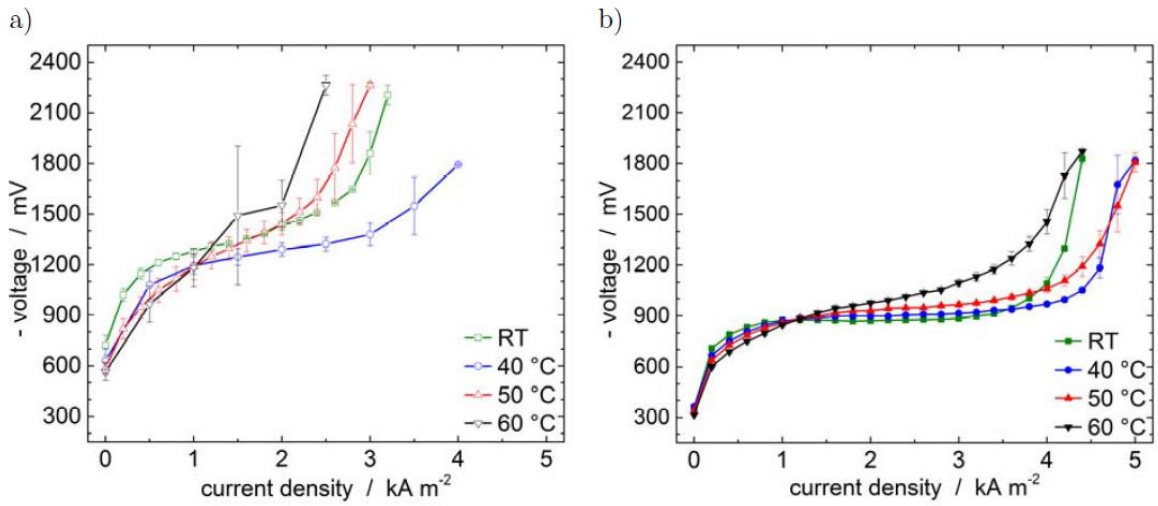

Figure 7. Current-cell potential curves employing membranes pretreated in $HCl_{(aq)}$ (a) and in H_2SO_4 (b) at different temperatures and a cathode humidification of 100 % . Reprinted from [19] with permission from Springer Nature.

As discussed above, the cell performance is significantly enhanced by utilizing H_2SO_4 for the membrane pretreatment and therefore (Fig. 7b) is chosen for the further discussion of the second critical influence on the cell performance, the water management. For all investigated temperatures, a limiting behavior can be observed in (Fig. 7b) at current densities between 2.7 and 4 kA m^{-2}. The experimental data of Martinez *et al.* [20,21] and Kuwertz *et al.* [19,30] indicate that the underlying reasons are the flooding of the CCL and the dehydration of the ACL as well as the adjacent membrane area. As will be discussed in the following, process parameters like the humidification of the oxygen feed and the temperature, as well as structural parameters like the hydrophobicity of the GDL and the Nafion content of the CCL determine which one of the two effects predominates. As (Fig. 7b) shows, the limiting current density is highest at an intermediate temperature of 40°C. If only flooding of the cathode side and the associated mass transport limitations would limit the cell performance, one would expect the highest temperature of 60°C to be optimal, since then the saturation pressure of water at which condensation occurs as well as the mass transfer rate of water away from the CCL increases. Additionally, the reaction kinetics are accelerated by an increase in temperature. However, the highest temperature leads to the worst performance experimentally, which can be explained with the dehydration effect at the anode side leading to a drastic decrease in the proton conductivity in the ACL and adjacent membrane. This correlation already becomes obvious at intermediate current densities in the ohmic regime in (Fig. 7b). At lower temperatures, the potential almost remains constant

with increasing current densities in an interval from 1-3.5 kA m^{-2}, while the expected roughly linear increase is only found in the 60°C case. A likely explanation for this effect is the rising membrane humidification due to the water emerging from the ORR at lower temperatures, increasing the proton conductivity of the membrane. At higher temperatures however, the generated water seems insufficient to further hydrate the membrane and therefore a steeper increase in the ohmic resistance can be observed in the interval from 1-3.5 kAm^{-2}. It has to be considered after all, that the dissociation of hydrogen chloride in the ACL is a highly exothermic reaction that, especially at already increased reactor temperatures, would facilitate the evaporation of water in the ACL and adjacent membrane. At the same time, the condensation of water in the CCL at higher current densities leads to a blockage of pore structures followed by a steep increase in the mass transfer resistance, which explains the lower limiting current density of the room temperature measurement compared to the ones at intermediate temperatures.

These findings are supported by measurements of the half-cell potentials by Kuwertz *et al.* [19] at different humidities of the cathode feed stream. For the anode side, the lowest overpotential by far could be achieved with 100% humidification while intermediate values of 60-80% turned out to be optimal for the cathode [19], underlining again the challenge of dehydration on the anode side and flooding of the catalyst layer on the cathode side. Additionally, in the half-cell measurements of Martinez *et al.* [18,21], in which the cathode compartment was filled with liquid water, the limiting current density of the hydrogen chloride oxidation reaction was significantly higher compared to the experiments of Kuwertz employing the full cell with an ODC and no liquid water supply to the cathode. Furthermore, the best performance was achieved at the highest temperature of 60°C, indicating that presence of liquid water in the cathode compartment in the half cell of Martinez *et al.* [18,21] prevented the dehydration of the ACL that was observed in the experiments of Kuwertz *et al.* [19], as discussed above. This again is a sign for the importance of sufficient membrane and ACL hydration for the limiting behavior of the complete electrolyzer cell investigated by Kuwertz *et al*. [19]. This, and the fact that the complete electrolyzer performed worst at the highest temperature, indicates that if mechanism A (please see Sect. 1.4) is valid, the expected limiting current of the Tafel reaction is clearly greater than the observed limiting current in the complete electrolyzer cell of Kuwertz *et al.* and is therefore unlikely to influence the performance.

Moreover, Martinez *et al.* [20] showed that the optimal Nafion loadings are significantly smaller in the CCL compared to the ACL indicating again the significance of the flooding and dehydration effect. Lastly, Kuwertz *et al.* [28] found that a higher hydrophobicity of the GDL had almost no effect on the anode overpotential, however the least hydrophobic GDL lead to a markedly lower overpotential on the cathode side. The authors have explained this with a decreasing ability of the GDL to transport water away from the CCL to the gas channel with an increase in the hydrophobicity, which in turn facilitates the flooding of the catalyst layer. For further experiments pointing towards the significance of both discussed effects, the reader may refer to [18,19,20,30].

Closing this section it should be noted that the cathode overpotential contributes most to the overall potential loss. According to Kuwertz *et al.* [30], a potential loss of up to 750 mV at 3 kA m^{-2} can be assigned to the cathode reaction, which is three to five times higher than the one of the membrane and the anodic oxidation reaction combined [30]. This finding underlines the significance of the ORR and its further optimization under the complex influence of the simultaneous anodic oxidation of HCl leading to undesired membrane dehydration effects and the presence of chloride anions in the CCL.

In the following, the novel separation problem that comes hand in hand with the gas phase reactor is discussed and the efficiency of the overall process consisting of the gas phase reactor and different separation strategies are evaluated and compared to the Bayer UHDENORA variant.

2. Investigation and exergetic analysis of an overall process based on the gas phase reactor

2.1 Separation strategies in combination with the gas phase reactor

The anode outlet stream of the electrochemical gas phase reactor investigated by Kuwertz *et al.* [13] and Martinez *et al.* [18] consists mostly of chlorine and unreacted hydrogen chloride. Contrary to the liquid phase reactor in the Bayer UHDENORA process, the only source for water in the anode outlet stream is due to crossover through the membrane. These water traces, if significant, can be simply separated by cooling and thereby condensing the water, leaving only a

mixture of HCl and Cl_2 to be separated. This new separation problem allows for different and more energy efficient separation strategies compared to the Bayer UHDENORA process, as Bechtel *et al.* [7,36,37] showed. The authors investigated three possible approaches for separating the chlorine that can be combined with the gas phase reactor and carried out flowsheet simulations as well as an exergy analysis of the three overall process variations in comparison to the state-of-the-art process. The simplified flowsheets of the three separation strategies combined with the electrochemical gas phase reactor are depicted in (Fig. 8). The three process variants are namely the ELECTRA-DIST, the ELECTRA-ABS and the ELECTRA-IL process as briefly discussed in the following. More detailed process flowsheets and further information on the proposed process variants can be found in [7,36].

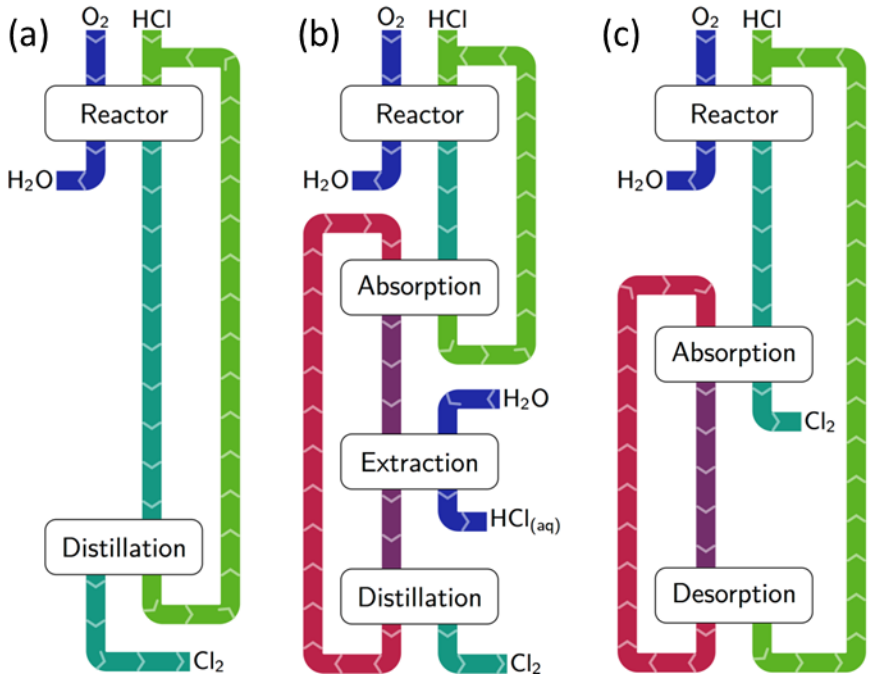

Figure 8. Simplified flowsheets of the ELECTRA-DIST (a), the ELECTRA-ABS (b), and the ELECTRA-IL (c) process. This graphic was kindly provided by Dr. Jörg Kluge, Max Planck Innovations, Munich.

The process variant ELECTRA-DIST (Fig.8.a) is based on a low temperature distillation at pressures between 1 and 10 bar. From the top of the column, HCl can be obtained and partly refed into the reactor as well as partly dissolved in water (not shown in Fig. 8a) to form concentrated hydrochloric acid as a byproduct in any desired ratio. The purified chlorine can directly be gained from the bottom of the distillation column [7].

The variant ELECTRA-ABS (Fig. 8b) combines an absorption with an extraction step. Various non-polar organic solvents show a higher selectivity for dissolving chlorine compared to HCl. However, for none of these solvents, the selectivity is high enough in order to not simultaneously absorb too much HCl in addition to the chlorine, so that the obtained product would not fulfill the purity standards. Hence, Bechtel *et al.* [7] proposed the following strategy. In a first step the HCl/Cl_2 mixture is brought into contact with the organic solvent in an absorption unit. Hereby, the chosen amount of solvent is just enough to dissolve all of the chlorine. Therefore, the gas stream leaving the absorber on top of the absorber consists of essentially pure HCl that can be refed into the electrochemical reactor. The solvent contains all chlorine and traces of HCl. These traces are subsequently separated in an extraction step with water. Due to the highly exergonic dissociation reaction of HCl in water, the organic solvent stream contains only chlorine and small traces of water after the extraction step. The chlorine is then desorbed from the solvent and the latter one is refed into the absorption column. The diluted hydrochloric acid obtained from the extraction is enriched with gaseous HCl from the top of the absorption column in order to form concentrated hydrochloric acid which is discharged as a byproduct. In the work of Bechtel *et al.* [7] octane was chosen as a solvent due to its low toxicity, cheap price and good availability. Other non-polar organic substances that are stable in the reactive HCl/Cl_2 environment at temperatures of up to 100°C can be selected as an alternative.

The final process variant, ELECTRA-IL (Fig. 8c), addresses the challenge of the low selectivity of classical organic solvents. Due to their polarity, certain ionic liquids (ILs) show a high selectivity and capacity for absorbing HCl in comparison to chlorine while being chemically stable in the aggressive environment of the present process. Hence, an IL is proposed for absorbing the hydrogen chloride from the anode outlet stream at ambient temperature and atmospheric pressure, leaving essentially pure chlorine in the remaining gas stream. The absorbed HCl is subsequently desorbed by increasing the temperature and reducing the pressure.

After compressing the so obtained gaseous HCl and the IL back to atmospheric pressure, both can be recycled into the process. If desired, a part of the hydrogen chloride can be dissolved in water to form concentrated hydrochloric acid as a byproduct, as already discussed for the two previously described process variants. The most suitable IL can be found by an integrated design approach combining quantum chemical solvent screening with process flowsheet simulations proposed by Bechtel *et al.* [36,37], taking into consideration the chemical stability of the IL as well as physical and thermodynamic parameters. More details about this screening procedure and the overall process can be found in [36,37]. In the following, the exergetic efficiencies of all three process variants including the gas phase reactor as well as the according separation strategies in comparison to the Bayer UHDENORA process are delineated.

2.2 Exergetic analysis and comparison to the state-of-the-art

For the exergetic assessment of the different process variants, Bechtel *et al.* [7] chose the MDI production site of BASF SE in Antwerp with an MDI capacity of 650 kt per year as an example process. This production volume is equivalent to 375 kt per year of HCl emerging as a byproduct and subsequently being electrochemically converted to chlorine or dissolved in water forming concentrated hydrochloric acid in a desired ratio. Since the exergy of the substances entering and leaving the process is identical for all process variants including the state-of-the-art process, Bechtel *et al.* [7] compared the exergy of all involved utility streams, including heat, work and electricity. In (Tab. 1) the so calculated exergy demand of the three proposed processes, simulated with two different single pass conversions in comparison to the Bayer UHDENORA process, is shown [7].

The exergetic savings compared to the state-of-the-art process mount up to 36-38% depending on the process variant. Therefore, not only the electrochemical gas phase reactor but also the overall processes proposed by Bechtel *et al.* [7,36,37] show a significantly lower energy demand compared to the Bayer UHDENORA process based on the liquid phase reactor. While the exergy demand of the three novel processes is comparable, with the ELECTRA-DIST process being slightly more efficient, they differ in certain process parameters and hence possess individual advantages and disadvantages [7]. The ELECTRA-DIST variant for example consists of the least

amount of devices, however in order to condense the chlorine at the top of the distillation column, a more costly cooling cycle would be necessary in comparison to the two other process variants due to the low temperature. An advantage of the ELECTRA-ABS process over the other two variants is its insensibility to water traces in the anode outlet stream due to crossover through the membrane in the electrochemical reactor. If small amounts of water are present in the anode stream, they won't interfere with the subsequent process steps [7]. Lastly, the ELECTRA-IL process has the advantage of not needing any cooling streams below room temperature and the discharged heat being at a comparably high temperature level, which allows for a flexible and efficient use of the discharged heat in the production site. Therefore, the choice of one of the three proposed variants does not depend on their very similar exergetic efficiencies but rather on site specific criteria like the availability of an appropriate cooling network amongst others [7].

In (Fig. 9), the exergy demand is broken down to the contributions of the involved unit operations for the Bayer UHDENORA process in comparison to the ELECTRA-IL variant. The according diagrams for the two remaining process variants can be found in [34]. As expected, the graph shows a significantly lower exergy demand on the reactor level. Furthermore, it depicts the grave inefficiency of the distillation step in the Bayer UHDENORA process due to the high heat capacity of the dilute hydrochloric acid and the enormous recycle streams. In comparison, the exergy demand of the separation step in the ELECTRA-IL process is by 86% lower. A significant portion of the exergy employed in the distillation column of the state-of-the-art process can be regained through the subsequent heat exchangers, depicted in form of the negative bar in (Fig 9). However, the discharged heat has a temperature level of only around 100-110°C and is therefore not usable in many real chemical production sites, meaning it would simply be waste heat. In that case, the novel process variants based on the gas phase reactor would be even more advantageous compared to the Bayer UHDENORA process.

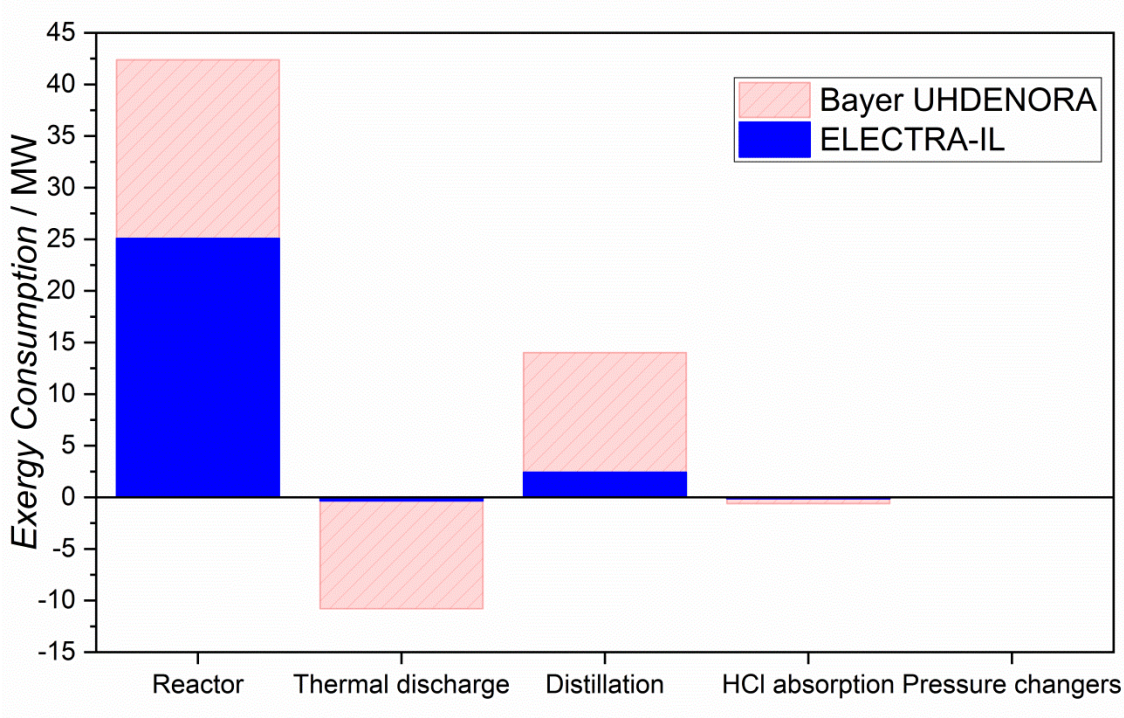

Figure 9. Exergy demand of the single unit operations in the ELECTRA-IL process (blue, filled) in comparison to the Bayer UHDENORA process (red, shaded). Adopted from [36].

As already foreseeable from (Fig. 9), the electrochemical reactor has by far the highest exergy demand of all unit operations in the overall process, especially in the case of the process variants based on the gas phase reactor due to their significantly more efficient separation strategies. This correlation is further visualized in the Sankey diagram (Fig. 10), which depicts the chemical and physical exergy flows as well as the exergy of the supplied utilities exemplary for the ELECTRA-DIST process.

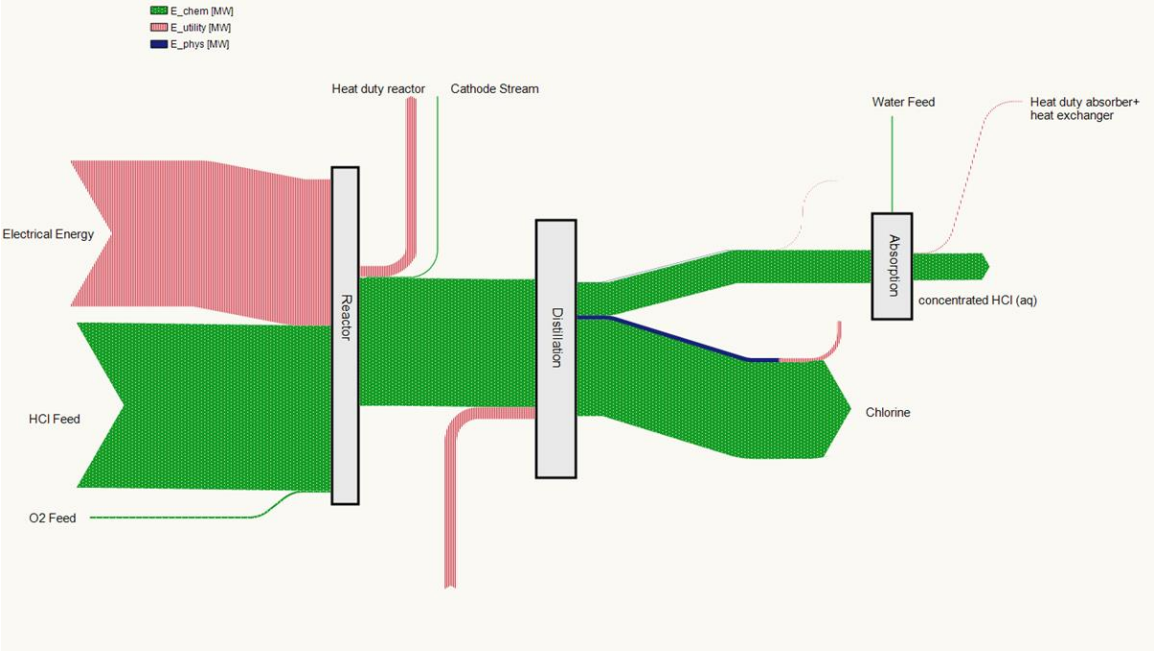

Figure 10. Sankey diagram for the ELECTRA-DIST process with a single pass conversion of 80 %. The physical and chemical exergy flows of each stream are depicted in blue and green respectively, while the exergy flows of the incoming and outgoing heat and work streams are displayed in red. The physical exergy is negligible in all streams except for the liquid chlorine leaving the bottom of the distillation column (blue line emerging from the distillation unit). Adapted from [7] with permission from Elsevier B.V.

While the investigation of feasible separation strategies is critical for the industrial applicability of the proposed processes, (Fig. 10) shows clearly that the major optimization potential does not lie within the separation strategies but within the reactor itself. Hence, future investigations on the development of the electrolysis of gaseous HCl should focus on further optimizing the electrochemical reactor, which would lead to an almost proportional increase in the overall process efficiency [7]. Future challenges in this field are certainly the water and thermal management in the reactor to avoid flooding on the one hand and dehydration of the ACL and membrane on the other hand as well as a suitable catalyst system and the prevention of HCl/Cl_2 crossover.

Summary

The growing production volumes of polyurethanes among others, contributing to an oversaturated market for the emerging HCl, require for a sustainable and feasible utilization of this byproduct. The recycling of HCl to chlorine, either heterogeneously catalyzed at high

temperatures, or by means for electrolysis, is a promising and long practiced approach to this challenge. The electrolysis of HCl was industrially established in the 1960s. The up to now most efficient industrially employed electrochemical process, the Bayer and UHDENORA process, is based on a liquid phase membrane reactor utilizing hydrochloric acid as a feedstock. Recently, investigations on an electrochemical gas phase reactor utilizing an ODC showed significant exergy savings compared to the state-of-the-art liquid phase reactor of up to 36 %. It turned out that the most critical features of this novel gas phase reactor are the performance of the cathode, being strongly influenced by the crossover of HCl/Cl_2 and a subsequent poisoning of the cathode catalyst, as well as the water management at technical current densities. In the latter case, the challenge is to balance the two opposing effects of the dehydration of the ACL and adjacent membrane on the one hand and the flooding of the CCL due to a liquid water excess on the other hand. Hereby, the dehydration of the ACL is possibly facilitated by the strongly exothermic dissociation reaction of HCl in the water containing Nafion of the catalyst layer. Hence, further studies should aim on a better understanding of the transport processes of water as well as HCl/Cl_2 through the membrane and the non-isothermal behavior of the reactor. Additionally, research was done in the field of electrode kinetics for the HCl oxidation reaction. While some light was shed on a possible reaction mechanism, further research is necessary and should include the investigation of the dissociation of HCl in the water containing ionomer in the anode catalyst layer.

In addition to the significant exergy savings on the reactor level compared to the state-of-the-art liquid phase reactor, the gas phase reactor also allows for a more efficient separation strategy. So far, three process variants based on the gas phase reactor and different separation sequences were proposed. Their overall exergy demand is reduced by 36-38 % compared to the Bayer UHDENORA process. The analysis furthermore showed that in all of the investigated process variants, the electrochemical reactor plays by far the most important role when considering the contribution of the individual unit operations to the overall exergy demand. Hence, while investigating the separation problem is of great importance for evaluating the industrial applicability of the process, further attempts to increase the overall efficiency should focus on the electrochemical reactor. In conclusion, the gas phase reactor for the electrolysis of HCl in combination with more efficient separation strategies is a promising and more feasible alternative to the current state-of-the-art process based on a liquid phase reactor.

Acknowledgement

The author Simon Bechtel is also affiliated to the International Max Planck Research School (IMPRS) for Advanced Methods in Process and Systems Engineering, Magdeburg, Germany.

Table of Contents

The electrochemical oxidation of HCl to Cl_2 plays a significant role in production of polycarbonates and polyurethanes. While the currently industrially implemented electrolysis processes all rely on a liquid phase reactor, recent investigations have shown that employing a gas phase reactor leads to enormous exergetic savings. This article outlines the concept of the energy efficient electrolysis of gaseous HCl on the reactor and overall process level.

References

1 M. F. Sonnenschein, *Polyurethanes Science, Technology, Markets and Trends,* 1st ed., Wiley, Hoboken, New Jersey, **2015**.

2 http://www.eurochlor.org/media/9385/3-2-the_european_chlor-alkali_industry_-_an_electricity_intensive_sector_exposed_to_carbon_leakage.pdf (Accessed on December 22, 2017).

3 https://issuu.com/jswapn23/docs/chlorine_market_worth (Accessed on November 10, 2017).

4 J. Perez-Ramirez, C. Mondelli, T. Schmidt, O. F. Schlüter, A. Wolf, L. Mleczko, T. Dreier, *Energy Environ Sci.* **2011**, *4*, 4786–4799. DOI: 0.1039/c1ee02190g

5 http://www.digitalrefining.com/data/literature/file/869775969.pdf (Accessed on August 21, 2018).

6 https://mcgroup.co.uk/news/20150505/tdi-manufacturers-europe-restructure-expand-production-capacities.html (Accessed on June 25, 2017).

7 S. Bechtel, T. Vidakovic-Koch, K. Sundmacher, *Chem. Eng. J.* **2018**, *346*, 535-548. DOI: 10.1016/j.cej.2018.04.064

8 J. Jörrisen, in Encyclopedia of Applied Electrochemistry (Eds: G. Kreysa, K. Ota, R. F. Savinell), 2014 ed., Springer Science+Business Media, New York 2014.

9 https://www.thyssenkrupp-uhde-chlorine-engineers.com/en/products/hydrochloric-acid-recycling/odc-technology/benefits-of-the-odc-technology/ (Accessed on March 14, 2019).

10 P. Ooms, A. Bulan, (Bayer Material Science AG), *European Patent 2371807 A1*, **2010**.

11 T. Vidakovic-Koch, I. G. Martinez, R. Kuwertz, U. Kunz, T. Turek, K. Sundmacher, *Membranes* **2012**, *2*, 510-528. DOI: 10.3390/membranes2030510

12 J. A. Trainham, C. G. Law, J. S. Newman, K. G. Keating, D. J. Eames, *US Patent 5411641 A*, **1995.**

13 R. Kuwertz, I. G. Martinez, T. Vidaković-Koch, K. Sundmacher, T. Turek, U. Kunz, *Electrochem. Commun.* **2013**, *34*, 320-322. DOI: 10.1016/j.elecom.2013.07.035

14 Y. Zhao, S. Gu, K. Gong, J. Zheng, J. Wang, Y. Yan *Angew. Chem. Int. Ed.* **2017**, *56, (36)*, 10735-10739. DOI: 10.1002/anie.201704749

15 Y. Zhao, S. Gu, K. Gong, J. Zheng, J. Wang, *J. Electrochem. Soc*. **2017**, *164, (7)*, E138-E143. DOI: 10.1149/2.0461707jes

16 P. Tatapudi, J. M. Fenton, *Proc. Electrochem. Soc. 1995, 95, (11)*, 252-265.

17 K. Hongsirikarn, J. G. Goodwin, S. Greenway, *J. Power Sources* **2010**, *195, (21)*, 7213-7220. DOI: 10.1016/j.jpowsour.2010.05.005

18 I. G. Martinez, *Elektrolyse von Chlorwasserstoff in einem Polymerelektrolyt-Membranreaktor mit Sauerstoffverzehrkathode*. Ph.D. Thesis, Otto-von-Guericke-Universität Magdeburg **2015.**

19 R. Kuwertz, I. G. Martinez, T. Vidaković-Koch, *J. Appl. Electrochem*. **2016**, *46, (7),* 755-767. DOI: 10.1007/s10800-016-0966-9

20 I. G. Martinez, T. Vidaković-Koch, R. Kuwertz, U. Kunz, T. Turek, K. Sundmacher, *Electrochim. Acta* **2014**, *123,* 387-394. DOI: 10.1016/j.electacta.2014.01.050

21 I. G. Martinez, T. Vidaković-Koch, R. Kuwertz, U. Kunz, T. Turek, K. Sundmacher, *J. Serb. Chem. Soc.* **2013**, *78,* 2115-2130. DOI: 10.2298/JSC131119142G

22 D. J. Eames, J. Newman, *J. Electrochem. Soc.* **1995**, *142, (11),* 3619-3625. DOI: 10.1149/1.2048388

23 C. M. Lai, J. C. Lin, F. P. Ting, S.-D. Chyou, K.-L. Hsueh, *Int. Hydrog. Energy* **2008**, *33, (15),* 4132-4137. DOI: 10.1016/j.ijhydene.2008.05.074

24 K. H. Kim, K. Y. Lee, H. J. Kim, E. Cho, S. Y. Lee, T. H. Lim, S. P. Yoon, I. C. Hwang, J. H. Jang, *Int. J. Hydrogen Energy* **2010**, *35, (5),* 2119–2126. DOI: 10.1016/j.ijhydene.2009.11.058

25 V. S. Bagotzky, Y. B. Vasslilyev, J. Weber, J. N. Pirtskhalava, *J. Electroanal. Chem.* **1970**, *27, (1),* 31-46. DOI: 10.1016/S0022-0728(70)80200-5

26 S. Gilman, *J. Phys. Chem.* **1964**, *68, (8),* 2098-2111. DOI: 10.1021/j100790a013

27 I. V. Zenyuk, P. K. Das, A. Z. Weber, *J. Electrochem. Soc.* **2016,** *163***,** *(7),* F691-F703. DOI: 10.1149/2.1161607jes]

28 L. Xing, X. Liu, T. Alaje, R. Kumar, M. Mamlouk, K. Scott, Energy **2014**, *73,* 618-634. DOI: 1 0.1016/j.energy.2014.06.065

29 H. A. Gasteiger, J. E. Panels, S. G. Yan, *J. Power Sources* **2004**, *127, (1-2)*, 162-171. DOI: 10.1016/j.jpowsour.2003.09.013

30 R. Kuwertz, N. Aoun, T. Turek, U. Kunz, *J. Electrochem. Soc.* **2016**, *163, (9)*, F988-F997. DOI: 10.1149/2.0261609jes

31 T. J. Schmidt, U. A. Paulus, H. A. Gasteiger, R. J. Behm, *J. Electroanal. Chem.* **2001**, *508*, 41-47. DOI: 10.1016/S0022-0728(01)00499-5

32 R. Kuwertz, C. Kirstein, T. Turek, U. Kunz, *J. Membrane Sci.* **2016**, *500*, 225-235. DOI: 10.1016/j.memsci.2015.11.022

33 I. Katsounaros, W. B. Schneider, J. C. Meier, U. Benedikt, P. U. Biedermann, A. Cuesta, A. A. Auer, K. J. Mayrhofer, *Phys. Chem. Chem. Phys.* **2013**, *15*, 8058—8068. DOI: 10.1039/c3cp50649e

34 J. X. Wang, N. M. Markovic, R. R. Adzik, *J. Phys. Chem. B* **2004,** *108, (13)*, 4127-4133. DOI: 10.1021/jp037593v

35 R. J. Allen, J. R. Giallombardo, D. Czerwiec, E. S. Castro, K. Shaikh, F. Gestermann, H.-G. Pinter, G. Speer, *US Patent 6402930B1*, **2002**.

36 S. Bechtel, Z. Song, T, Zhou, T. Vidakovic-Koch, K. Sundmacher, in *Proc. of the 13th Intern. Symp. on Process Systems Engineering –PSE 2018 Part A* (Eds: M. R. Eden, M. G. Ierapetritou), Elsevier B.V. Amsterdam **2018.**

37 S. Bechtel, T. Vidakovic-Koch, K. Sundmacher, *European Patent 17203967.9*, handed in on **28.11.2017.**

Table 1. Overall exergy demand of the ELECTRA-DIST, ELECTRA-ABS, ELECTRA-IL and Bayer UHDENORA process. In all simulations the overall conversion of HCl to chlorine was arbitrarily set to 80 % and the remaining HCl was dissolved in water forming concentrated hydrochloric acid for reasons of comparability. In order to investigate the influence of the single pass

conversion on the efficiency of the process, two different exemplary single pass conversions were simulated for the ELECTRA-DIST and –ABS process. The Data in Table 1 is based on [7,36,37].

Process variant	Exergy consumption / MW
State-of-the-art	42.30
Process ELECTRA-DIST at 80 % single pass conversion	26.26
Process ELECTRA-DIST at 60 % single pass conversion	26.45
Process ELECTRA-ABS at 80 % single pass conversion	27.04
Process ELECTRA-ABS at 60 % single pass conversion	28.39
Process ELECTRA-IL at 80 % single pass conversion	27.00

Figure Legends

Figure 1. Utilization of electrical energy, for example from renewable sources, for the electrolysis of gaseous HCl emerging from processes like the isocyanate and, for certain process variants, the polycarbonate production. The obtained chlorine can then be refed into these production processes. Reprinted from [7] with permission from Elsevier B.V.

Figure 2. Process flowsheet of the Bayer UHDENORA process. Reprinted from [7] with permission from Elsevier B.V.

Figure 3. Scheme of the gas phase reactors as proposed by Kuwertz *et al.* [13] (a), Dupont [12] (b) and Zhao *et al*. [14,15,16] (c).

Figure 4. Thermodynamic efficiency (a) and reversible equilibrium cell potentials (b) for the four different discussed HCl electrolysis processes. Adopted from [18] with permission from author.

Figure 5. (a) Working principle of the gas phase reactor. Reprinted from [30] with permission from the Electrochemical Society. (b) Explosion view of a gas phase reactor for the hydrogen chloride electrolysis consisting of: One MEA (1), two GDLs (2), two bipolar plates (3), two end plate (4) and the gaskets (5). Reprinted from [19] with permission from Springer Nature.

Figure 6. Influence of temperature on the HCl oxidation presented as Tafel plot. For all temperatures, even though less clear at a temperature of 25°C, two different Tafel-slopes of *ca*.

30 mV dec^{-1} at more negative potentials and *ca*. 60 mV dec^{-1} at more positive potentials can be observed [18]. Reprinted from [18] with permission from the author.

Figure 7. Current-cell potential curves employing membranes pretreated in $HCl_{(aq)}$ (a) and in H_2SO_4 (b) at different temperatures and a cathode humidification of 100 % . Reprinted from [19] with permission from Springer Nature.

Figure 8. Simplified flowsheets of the ELECTRA-DIST (a), the ELECTRA-ABS (b), and the ELECTRA-IL (c) process. This graphic was kindly provided by Dr. Jörg Kluge, Max Planck Innovations, Munich.

Figure 9. Exergy demand of the single unit operations in the ELECTRA-IL process (blue, filled) in comparison to the Bayer UHDENORA process (red, shaded). Adopted from [36].

Figure 10. Sankey diagram for the ELECTRA-DIST process with a single pass conversion of 80 %. The physical and chemical exergy flows of each stream are depicted in blue and green respectively, while the exergy flows of the incoming and outgoing heat and work streams are displayed in red. The physical exergy is negligible in all streams except for the liquid chlorine leaving the bottom of the distillation column (blue line emerging from the distillation unit). Adapted from [7] with permission from Elsevier B.V.

Table of contents

In recent years the gas phase electrolysis of HCl to Cl_2 has been investigated in more detail and found to be very promising in comparison to the classical, industrially employed liquid phase reactor (state-of-the-art). This review aims on discussing the benefits and challenges of the gas phase electrolysis on a reactor and overall process level and relates the exergetic efficiency of this novel process to the state-of-the-art variant.

Graphical abstract

We recommend using Fig. 8 as a graphical abstract.